Determination of the optical properties of sol-gel-derived $Ba_xSr_{1-x}TiO_3$ thin film by spectroscopic ellipsometry

2001 J. Phys.: Condens. Matter 13 4065

(http://iopscience.iop.org/0953-8984/13/18/314)

J. Phys.: Condens. Matter **13** (2001) 4065–4074 www.iop.org/Journals/cm PII: S0953-8984(01)19672-4

Determination of the optical properties of sol–gel-derived $Ba_xSr_{1-x}TiO_3$ thin film by spectroscopic ellipsometry

H Y Tian[1], W G Luo[1,3], X H Pu[1], X Y He[1], P S Qiu[1], A L Ding, S H Yang[2] and D Mo[2]

[1] Laboratory of Functional Inorganic Materials, Chinese Academy of Sciences, 1295 Ding Xi Road, Shanghai 200050, People's Republic of China
[2] Department of Physics, Zhongshan University, Guangzhou 510275, People's Republic of China

E-mail: wglald@sunm.shcnc.ac.cn

Received 4 September 2000, in final form 15 November 2000

Abstract
The optical properties of amorphous and polycrystalline $Ba_xSr_{1-x}TiO_3$ (BST) thin films fabricated on Si(100) substrates by a sol–gel spin-coating technique were investigated by spectroscopic ellipsometry (SE). The spectrum of the extinction coefficient k was obtained by using the refractive index and structure parameters determined by SE in the photon energy range of 2.1–5.2 eV. A four-phase fitting model was employed to describe the optical properties of the BST thin films; the spectra of their optical constants and the band gap energy E_g were determined by means of optimization. In addition, the refractive index dispersion data related to the short-range-order structure of the films agreed well with the single-oscillation energy model. The dependence of the refractive index, k and E_g on annealing temperature were analysed. The variation of optical band gap energy with composition was investigated by changing the content of barium in the films.

1. Introduction

Ferroelectric thin films are very promising for a wide range of applications such as high dielectric constant capacitors, non-volatile memories with low switching voltage, infrared sensors and electro-optic devices [1]. Among these materials, $Ba_xSr_{1-x}TiO_3$ (BST) has attracted much attention because of its unique combination of large dielectric constant, large electro-optical coefficient and low optical losses [2, 3]. There have been several reports on the electrical and optical properties of $BaTiO_3$, $SrTiO_3$, and BST thin films [4–6]. The BST films can be transformed into a paraelectric phase by controlling the Ba/Sr ratio, and can perform as a highly transparent insulating layer which has been used in electroluminescent devices [7]. The BST thin films or multilayer systems can be used in non-linear optical devices

[3] Corresponding author, fax: +86-21-62513903.

such as planar waveguides or optical switches with minimal optical propagation losses [8, 9]. Some authors have studied the optical properties of inhomogeneous oxide films fabricated by different techniques, while assuming a linear variation in the refractive index along the thickness of the films [10, 11]. In the inhomogeneous layer, a void distribution has been assumed to vary instead of the refractive index [12].

The ellipsometric determination of the optical constants of inhomogeneous BST thin films derived from a sol–gel technique, to our knowledge, has not been mentioned yet in the literature. In our research, spectroscopic ellipsometry (SE), known to be a very useful and non-destructive technique for investigating the optical properties of transparent ceramic films, has been used to analyse the optical properties related to temperature and composition.

2. Experimental procedure

In our experiment BST thin films were prepared by a sol–gel technique with barium acetate $Ba(CH_3CO_2)_2$, strontium acetate $Sr(CH_3CO_2\cdot 1/2H_2O)_2$ and tetrabutyl titanate $Ti(OC_4H_9)_4$ as starting materials. Acetic acid and methanol were selected as solvents, ethylene glycol dimethyl ether as additives, and acetyl acetone as a reagent to stabilize the tetrabutyl titanate. Barium acetate and strontium acetate were mixed in a desired ratio of Ba/Sr, e.g., $Ba_{0.9}Sr_{0.1}TiO_3$(90/10), then dissolved into heated acetic acid containing equimolar amounts of titanium butoxide which was stabilized by an appropriate amount of acetylacetone. Details of the sol–gel process and its use for the deposition of the ferroelectric thin films may be found elsewhere [13].

The ellipsometric spectra of the samples were measured by a home-made automatic rotating analyser type ellipsometer in the wavelength range of 240–600 nm. The angle of incidence was 70 °, and the azimuth of polarization 45 °.

3. Results and discussion

Spectroscopic ellipsometry is an optical technique used to measure the ratio of the complex Fresnel reflection coefficients

$$\rho = \tan\Psi e^{i\Delta} = \frac{R_p}{R_s} = \left|\frac{R_p}{R_s}\right| \exp[i(\delta_p - \delta_s)] \quad (1)$$

where the complex Fresnel reflection coefficients R_p and R_s correspond to the parallel and perpendicular components, respectively. The values of $\tan\Psi$ and $\cos\Delta$ of the ellipso-metric parameters are measured for each wavelength by Fourier analysing a variation of the light intensity versus the azimuth of the analyser. The spectra for BST thin films annealed from 500 to 730 °C are shown in figures 1(a)–(c). The optical constants derived from the ellipsometric parameters of $\tan\Psi$ and $\cos\Delta$ are analysed by a four-phase model, as shown in figure 2.

In our research, a four-phase model (air/BST+voids/BST/substrate) has been used to fit the SE data, taken in the photon energy range of 2.1–5.2 eV. The presence of a high percentage of voids is a common feature for sol–gel-derived oxide thin films [12]. In the surface layer, there is a large number of voids with almost 44% of air volume. From analysis of the atomic force microscope (AFM) image of our BST (90/10) thin film, the rms roughness and the maximum roughness height were found to be 3.4 and 16.2 nm, respectively, for the surface region of 500 nm × 500 nm area. The thickness of the film was about 92 nm derived from Dektak^{3}st surfacefiler (Veeco Instruments Inc., USA).

A four-phase model was used to analyse the ellipsometric spectra. The refractive index and extinction coefficient as functions of the photon energy as well as the film thickness were determined by fitting the ellipsometric spectra using an optimization algorithm. The refractive

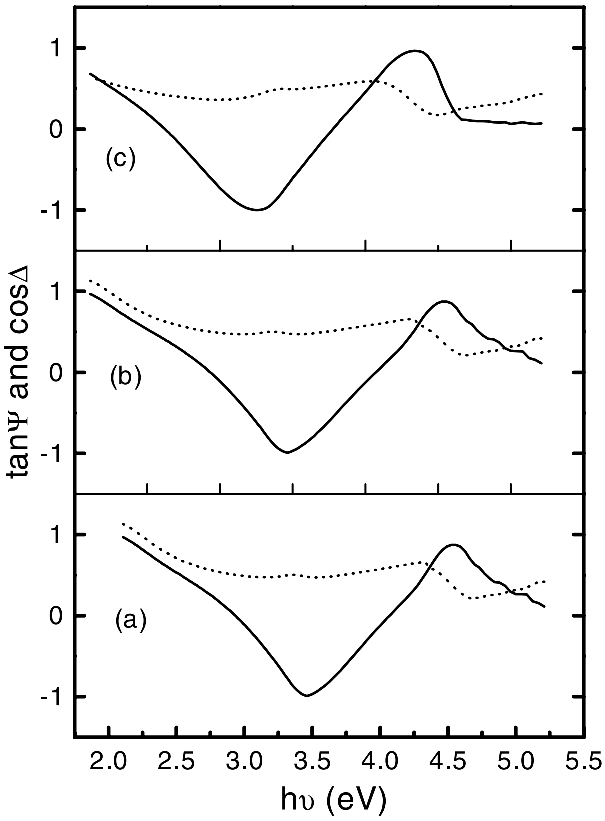

Figure 1. Ellipsometric spectra of $Ba_{0.9}Sr_{0.1}TiO_3$ thin films annealed at various temperatures (a) 500 °C, (b) 600 °C and (c) 730 °C.

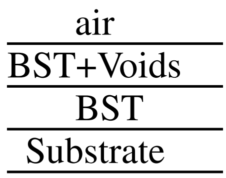

Figure 2. Schematic diagram of the film structure used in SE fitting.

index first increased and then decreased as the photon energy increased from 2.0 to 5.2 eV, as shown in figure 4. We also found that the refractive index increased as the annealing temperature increased from 500 to 730 °C, being equal to 1.99 at 500 °C, 2.08 at 600 °C, and 2.18 at 730 °C for a wavelength of 624 nm. A higher annealing temperature not only increases the mobility of atoms or molecules of the films, but also enhances the formation of larger and more closely packed crystals. The increase of the refractive index with increasing temperature can be partly attributed to the decrease of the density of voids in the films.

Didomenico and Wemple [14] have shown that the electro-optical properties of ferroelectrics may be simply expressed in terms of an effective polarization potential associated with the lowest-energy interband transition. It is a very useful approach to analyse the

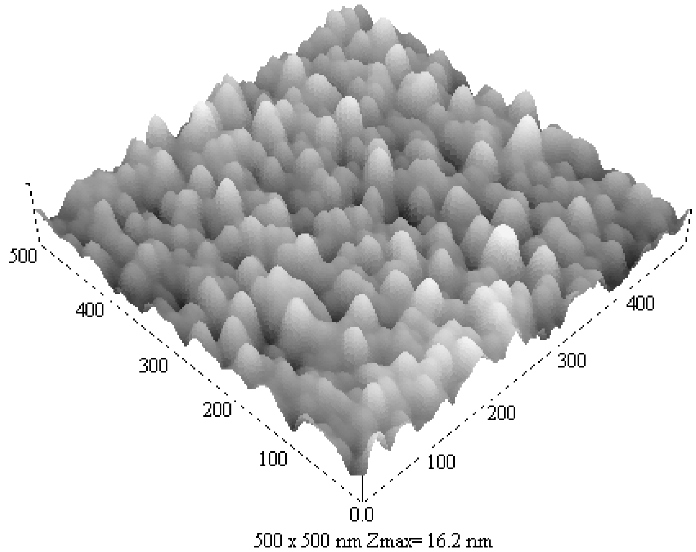

Figure 3. Three-dimensional surface morphology of the $Ba_{0.9}Sr_{0.1}TiO_3$ thin film obtained by AFM.

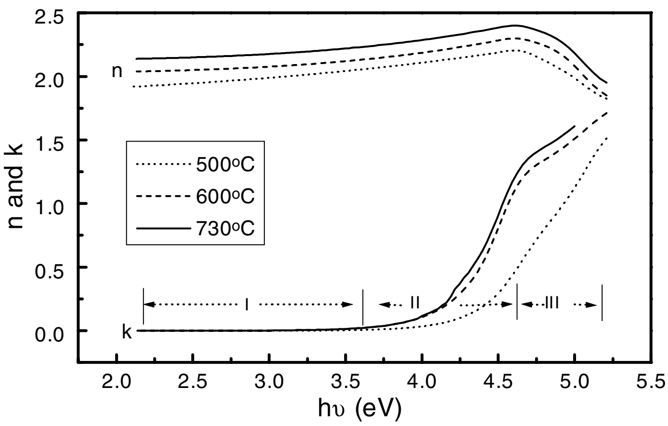

Figure 4. Optical constants (refractive index and extinction coefficient) as a function of photon energy of $Ba_{0.9}Sr_{0.1}TiO_3$ thin films annealed at 500, 600 and 730 °C, respectively.

ferroelectric thin film for the optical properties in our work. The similarity of the optical properties lies in the fact that the BO_6 octahedron governs the lower-lying conduction bands and the upper valence bands. Other ions in the structure contribute to the higher-lying conduction states, but these generally have only a small effect on the optical properties [15]. The lowest-energy oscillator is the largest contributor to the dispersion of the refractive index. For oxygen-octahedra in the BST thin film the lowest-energy oscillator corresponds to excitations to the B-cation d-electron t_{2g} band; the band gap energies are 4.33 eV for 500 °C, 4.14 eV for 600 °C and 4.11 eV for 730 °C, respectively. Further increase of the photon energy will result in decrease of the refractive index, with turning points around 4.6 eV for all samples, which is slightly smaller than those derived from figure 5.

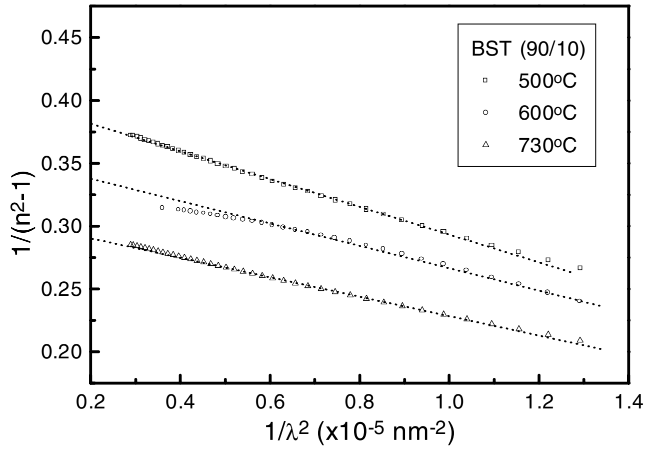

Figure 5. Dependence of $1/(n^2-1)$ on $1/\lambda^2$ for $Ba_{0.9}Sr_{0.1}TiO_3$ thin films annealed at various temperatures.

The extinction coefficient spectra for the BST (90/10) thin films annealed at different temperatures are also shown in figure 4. From the spectral relationship between extinction coefficient and photon energy, the extinction coefficient of the BST thin films can be divided into three regions; region I: the low-energy region of the spectra ($E = 2.1$–3.7 eV, below the fundamental band gap energy E_g); regions II and III: the high-energy region ($E = 3.7$–4.6 and 4.6–5.2 eV, above E_g). No obvious absorption is found below the fundamental band gap energy, so the extinction coefficient is near to zero except when the photon energy increased close to the band gap energy. The dispersion peaks in regions II and III are due to the transition from the valence band to the conduction band, or a transition from a band to an impurity level. The values of the extinction coefficient, as we know, result from the absorption and grain scattering when the photon wavelength is equivalent to the grain size in the high-energy region. The possibility of scattering of the grains increases as the temperature increases, which can also be attributed to the increase of grain size and surface density of the films. The extinction coefficient near the fundamental band gap energy is not zero because of the noise, and the results demonstrate that some other absorption is present in addition to the fundamental transition. It is interesting that there is a point of inflection in the extinction coefficient curves, where the rate of increase of the coefficient slackens. This corresponds to the turning points of the refractive index around a photon energy of 4.59 eV. This result is in good agreement with that of Kim *et al* for the simultaneous determination of the optical parameters of TiO_2 thin film, where they reported similar spectra for the refractive index and extinction coefficient derived from SE characterization [16]. There is an inverse U shape that is highest in the middle and lowest at either the air–film or the film–substrate interface. Therefore, $\delta n = n_{\mathrm{air/film}} - n_{\mathrm{film/substrate}}$ of this film could be considered to be positive if one neglects the surface micro-roughness layer which is much thinner than the other layers.

To analyse the optical parameters, such as the oscillator and dispersion energies, the single-oscillator model was used in which the dispersion of the refractive index is related to the photon energy, $E = h\nu$, according to the equation [17],

$$n^2(E) = 1 + \frac{E_m E_d}{E_m^2 - E^2} = 1 + \frac{E_m E_d}{E_m^2 - (hc/\lambda)^2} \qquad (2)$$

where c denotes the speed of light, h is Planck's constant, E_m the single-oscillator energy and E_d the dispersion energy. These parameters can be easily obtained by plotting $1/(n^2 - 1)$ versus $1/\lambda^2$ of the BST thin films. The dependence of $1/(n^2 - 1)$ on $1/\lambda^2$ for $Ba_{0.9}Sr_{0.1}TiO_3$ thin films annealed at various temperatures is shown in figure 5. The parameters E_m and E_d are deduced from the slope of the resulting straight fitting line and from the infinite wavelength intercept, respectively. We can thus see the dependence of the dispersion parameters E_m and E_d on the annealing temperature. The value of the oscillator energy E_m is found to be 4.9 eV for the $Ba_{0.9}Sr_{0.1}TiO_3$ film annealed at 730 °C, decreasing from 5.2 eV to 4.9 eV as the annnealing temperature increased from 500 to 730 °C. On the other hand, E_d has an obvious increase from 18.3 eV to 23.1 eV as the annealing temperature increases from 500 to 730 °C. The values are slightly smaller than those obtained by Kuo *et al* [18] and Thielsch *et al* [19]. The different values may be partly attributed to the different crystalline structure and composition. It is reasonable to surmise that the oscillation and dispersion energies are strongly influenced by the actual film configuration so that films with a small amount of amorphous phase would have a higher E_m value. The dispersion curves follow the law: $n^2 - 1 = (Ne^2/m\varepsilon_o)(\omega_o^2 - \omega^2)^{-1}$ [20], and extrapolation of a plot of $1/(n^2 - 1)$ against $1/\lambda^2$ is the best way of determinating the refractive index n_o, where the n_o is the constant refractive index at the wavelengths well above the abosorption edge. The factor n_o^2 is also referred to as the high-frequency dielectric constant, and is in general different from the static or low-frequency (i.e. non-optical) dielectric constant ε_o. The values of n_o in our work increase monotonically from 1.86 to 2.07, as the annealing temperature increases from 500 to 730 °C.

The refractive index of the transparent ceramic thin films is directly correlated to the densification of the layer, the microstructure, and the crystalline state. The experimental values of the refractive index are found to fit closely to a Cauchy function of the form: $n(\lambda) = a + b/\lambda + c/\lambda^2$ with $a = 2.3350$, $b = -4.5870 \times 10^2$, and $c = 1.5111 \times 10^5$, where λ is the wavelength in nanometers. The dispersion data have also been interpreted with the single electronic oscillator model [17]. Figure 6 shows the relation between refractive index and wavelength for $Ba_{0.7}Sr_{0.3}TiO_3$ film. The dispersion curve is fairly flat above $\lambda = 550$ nm but rises rapidly toward shorter wavelengths, showing the typical shape of a dispersion curve near an electronic interband transition. The strong increase in the refractive index is associated with the fundamental band gap absorption. The absorption edge of the BST film (70/30) annealed at 730 °C is around 299 nm, as calculated from the SE data.

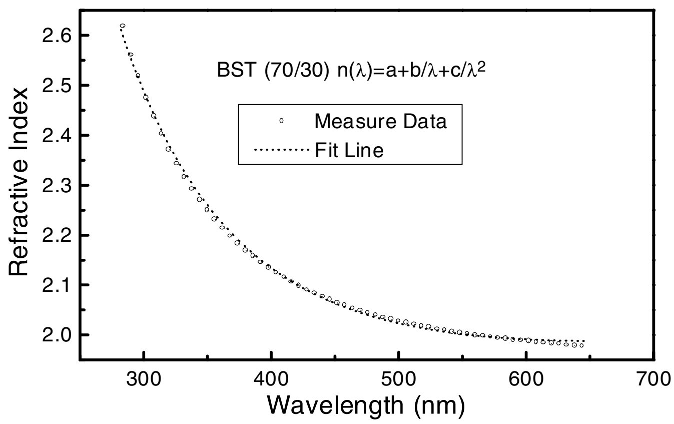

Figure 6. Refractive index as a function of wavelength for $Ba_{0.7}Sr_{0.3}TiO_3$ film.

The optical band gap energy of each film was deduced from the spectral dependence of the absorption constant $\alpha(\lambda)$ by applying the Tauc relation [21]:

$$\alpha(\lambda)h\nu = \text{const.} \times (h\nu - E_g)^{\frac{1}{r}} \quad (3)$$

where $r = 2$ for a direct allowed transition. The absorption $\alpha(\lambda)$ was determined from each transmittance spectrum using an extrema (or minima) envelope method, described in detail elsewhere [22]. The optical band gap was determined by extrapolating the linear portion of the plot to $(\alpha h\nu)^2 = 0$, thus supporting the direct allowed band model for deposition films. Figure 7 illustrates the optical band gap energy for $Ba_{0.8}Sr_{0.2}TiO_3$ films annealed at 730 °C, $E_g = 3.80$ eV. The calculated energy gap is higher than the energy gap (3.54 eV) of $Ba_{0.8}Sr_{0.2}TiO_3$ films derived from RF sputtering [6].

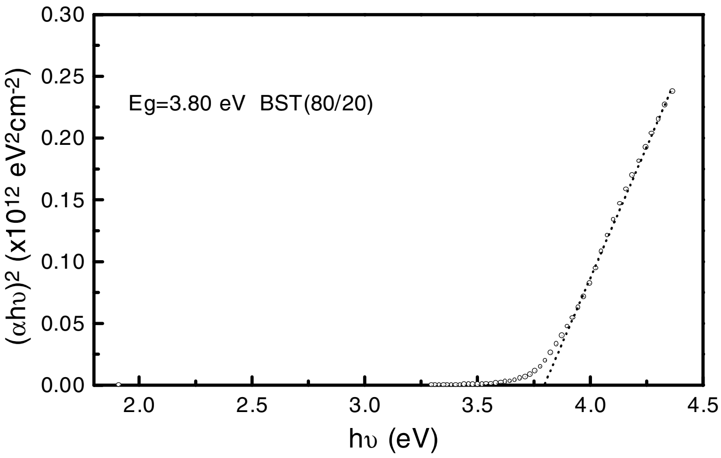

Figure 7. Plot of $(\alpha h\nu)^2$ versus $h\nu$ for $Ba_{0.8}Sr_{0.2}TiO_3$ film. The optical band gap energy E_g is deduced from extrapolation of the straight line to $(\alpha h\nu)^2 = 0$.

The optical band gap energy of the BST thin films is a composition-dependent parameter. Figure 8 shows the variation of the band gap energy with barium percentage in BST films. The band gap energy is found to decrease from 4.15 to 3.75 eV with increasing Ba/Sr ratio from 0.7 to 1.0. This is in agreement with the experimental results of composition-dependent band gap measurements of BST films reported in the literature [6]. When strontium is doped into barium titanate, Sr^{2+} ions will occupy the lattice site of the Ba^{2+} ions, which will enhance the coupling effect between the Ti^{4+} and O^{2-} ions because the effect of the Sr–O bond is stronger than that of the Ba–O bond. Furthermore, the lattice parameters will decrease with increasing strontium content in the BST thin films, due to the difference in radii of the Ba^{2+} ions ($r = 0.135$ nm) and Sr^{2+} ions ($r = 0.113$ nm). It is therefore more favourable to fabricate films with a higher packed density and less voids.

4. Conclusions

The optical properties of amorphous and polycrystalline BST thin films coated on Si(100) substrates by a sol–gel spin–coating technique have been investigated by spectroscopic ellipsometry. The extinction coefficient k spectrum has been obtained by using the refractive index and structure parameters determined by SE in the photon energy range of 2.1–5.2 eV. A four-phase fitting model was employed to describe the optical properties; the spectra of

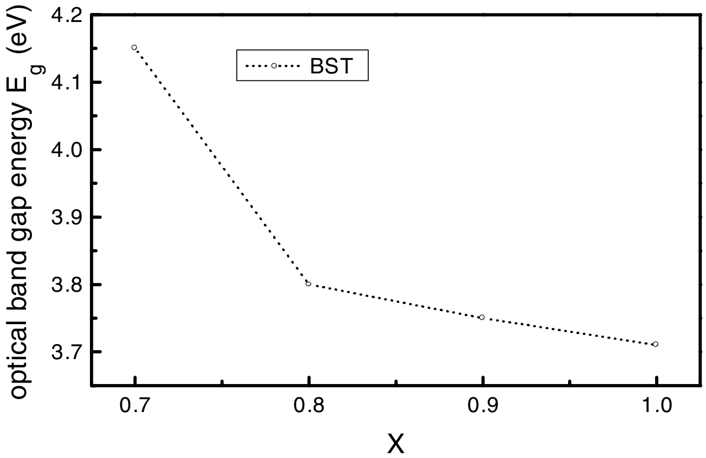

Figure 8. Optical band gap energies E_g of $Ba_xSr_{1-x}TiO_3$ films with various compositions (x denotes the content of Ba).

the optical constants and the band gap energy E_g were determined by means of optimization. The refractive index for $Ba_{0.9}Sr_{0.1}TiO_3$ increases from 1.99 to 2.18 at 624 nm as the annealing temperature is increased from 500 to 730 °C. The dispersion curve of $Ba_{0.7}Sr_{0.3}TiO_3$ film is fairly flat above $\lambda = 550$ nm, but rises rapidly toward shorter wavelengths, showing the typical shape of a dispersion curve near an electronic interband transition. The value of the oscillator energy E_m was found to be 4.9 eV for the $Ba_{0.9}Sr_{0.1}TiO_3$ film annealed at 730°C, decreasing from 5.2 eV to 4.9 eV as the temperature was increased from 500 to 730°C. The composition-dependent optical band gap was investigated by increasing the Ba/Sr ratio from 0.7 to 1.0, as a result of which the band gap decreased from 4.15 to 3.75 eV.

Acknowledgments

The authors would like to thank Dr Xingui Tang for many useful discussions. Financial support was provided by the National Natural Science Foundation of China (Grant No: 59995520) and the Laboratory of Functional Inorganic Materials of the Chinese Academy of Sciences.

References

[1] Xu Y H and Mackenzie J D 1992 *Integrared Ferroelectrics* **1** 17
[2] Hou S Y, Kwo J, Watts R K and Cheng J Y 1995 *Appl. Phys. Lett.* **67** 1387
[3] Yamamichi S, Yabuta H, Sukuma T and Miyasaka Y 1994 *Appl. Phys. Lett.* **64** 1644
[4] Kamalasanan M N and Chandra S 1991 *Appl. Phys. Lett.* **59** 3547
[5] Hohlecke M, Marrello V and Onton A 1997 *J. Appl. Phys.* **48** 1748
[6] Panda B, Dhar A, Nigan G D, Bhattacharga D and Ray S K, 1998 *Thin Solid Films* **332** 46
[7] Kim T S, Oh M H and Kim C H 1993 *Japan. J. Appl. Phys.* **32** 2837
[8] Gunther K H 1984 *Appl. Opt.* **23** 3612
[9] Granqvist C G and Hunderi O 1977 *Phys. Rev.* B **16** 3513
[10] Lariviere G P, Frigerio J M, Rivory J and Abeles F 1992 *Appl. Opt.* **31** 6509
[11] Borgogno J P, Flory F, Roche P, Schmitt B, Albrand G, Pelletier E and Macleod H A 1984 *Appl. Opt.* **23** 3567
[12] Raham M M, Yu G L, Krishna K M, Soga T, Wantanabe J J, Jimbo T and Umeno M 1998 *Appl. Opt.* **37** 691
[13] Tian H Y, Luo W G, Pu X H and Ding A L 2000 *J. Mater. Sci. Lett.* **19** 1211
[14] Dodomenico Jr M and Wemple S H 1969 *J. Appl. Phys.* **40** 720

[15] Lines M E and Glass A M 1977 *Principles and Applications of Ferroelectrics and Related Materials* (Oxford: Clarendon) p 497
[16] Kim S Y 1996 *Appl. Opt.* **35** 6703
[17] Dodomenico Jr M and Wemple S H 1969 *Phys. Rev. Lett.* **23** 1156
[18] Kuo Y F and Tseng Y 1991 *Materials Chemistry and Physics* **61** 244
[19] Thielsch R, Kaemmer K, Holzapfel B and Schultz L 1997 *Thin Solid Films* **301** 203
[20] Moss T S, Burrell G J and Ellis B 1973 *Semiconductor Opto-electronics* (London: Butterworth) p 25
[21] Tauc J C 1972 *Optical Properties of Solids* (Amsterdam: North-Holland) p 372
[22] Davis E A and Mott N F 1970 *Phil. Mag.* **22** 903